Effective Measures of "Effective" Discharge
Author(s): Lauren Klonsky and Richard M. Vogel
Source: *The Journal of Geology*, Vol. 119, No. 1 (January 2011), pp. 1-14
Published by: The University of Chicago Press
Stable URL: http://www.jstor.org/stable/10.1086/657258
Accessed: 05/01/2011 16:26

http://www.jstor.org

ARTICLES

Effective Measures of "Effective" Discharge

Lauren Klonsky[1],[*] *and Richard M. Vogel*[2]

1. CDM, Cambridge, Massachusetts 02139, U.S.A.; 2. Department of Civil and Environmental Engineering, Tufts University, Medford, Massachusetts 02155, U.S.A.

ABSTRACT

The concept of effective discharge, Q_e, was introduced by Wolman and Miller (1960) as that stream discharge that transports the most sediment over time. Recently, the validity of Q_e as an overall descriptor of sediment transport has been questioned because of its various interpretations and methods of calculation. A new discharge index—termed the "half-load discharge," $Q_{1/2}$—was introduced as the discharge above and below which half of the total sediment load has been transported over time. Existing methods along with long records of continuous daily suspended sediment and discharge data are used to clarify what a discharge index can accomplish. We also offer an objective and consistent empirical methodology for calculating Q_e based on a kernel density function. Generalized graphical relationships are introduced for summarizing the frequency and magnitude of both stream discharge and sediment loads. We document how Q_e and $Q_{1/2}$ are related to standard descriptors of river discharge as well as general characteristics of the sediment load-discharge relationship.

Introduction

Water is considered the dominant force in landscape alteration, which makes it a key component in understanding landscape evolution. The discharge indices described here, such as the effective discharge and the half-load discharge, enable fluvial geomorphologists and hydrologists to better understand the relationship between streamflow and sediment transport. Wolman and Miller (1960) first introduced the concept of effective discharge, Q_e, and nearly one-half century later, effective discharge is probably still the most widely used discharge index associated with the transport of suspended sediment. Evidence of the widespread use of Q_e is in part provided by the fact that there are now more than 550 citations to Wolman and Miller (1960). The effective discharge is often considered an index that describes the streamflow responsible for carrying the most sediment over time. Since its introduction, the interpretation, application, and even calculation of Q_e have not always been entirely clear or consistent. This led Vogel et al. (2003)

to introduce the half-load discharge, $Q_{1/2}$, which is defined as the discharge above and below which half of the total sediment load has been transported over time. The primary goals of this article are (1) to present a clear and consistent method of computing Q_e, (2) to introduce a generalized graphical approach for understanding and representing both discharge indices and the overall frequency and magnitude of sediment load volumes, and (3) to provide empirical comparisons of theoretical and regional relationships among discharge indices for a broad range of rivers across the United States.

A single discharge, known as the channel-forming discharge, is often used as the representative value for channel stability assessment and design. Although both Q_e and the bankfull discharge Q_b are widely considered estimates of the channel-forming discharge, Quader et al. (2008) cite numerous sources that recommend use of Q_e over Q_b as the channel-forming discharge. Q_e has also been used for many other applications, including quantification of channel maintenance flows, assessment of watershed disturbances, evaluation of flow regulation schemes for rivers, and support for

stream restoration (Bledsoe et al. 2007). Hudson and Mossa (1997, p. 263) suggest that Q_e is a "useful framework for understanding the timing and delivery of riverine sediments to the nearshore coastal environment from rivers draining a range of geologic and climatic change" as well as being helpful in analyzing "the transfer of fluvial sediment-associated pollutants into the nearshore zone." Orndorff and Whiting (1999) found Q_e to be a useful index for river restoration and maintenance projects. Doyle and Shields (2008) used Q_e to define an ecologically effective discharge, which is the discharge that drives the transport of organic matter, algal growth, nutrient retention, macroinvertebrate disturbance, and habitat availability.

Inconsistencies in estimation of Q_e exist as a result of numerous computational approaches advanced in previous studies. Most approaches to estimation of Q_e require some approximation of the probability distribution function (pdf) of daily streamflow. Historically, such methods involve a somewhat arbitrary binning of data. When computers were unavailable, binning of data was essential. However, binning methods are no longer necessary to approximate the empirical pdf of daily streamflow, nor do they provide a reproducible approach, because different investigators use different bin widths, leading to different results. For example, Doyle et al. (2005) divided a histogram into 25 bins in log space to represent the pdf of the daily discharge. Biedenharn et al. (1999) and Crowder and Knapp (2005) separated discharge data into 25 bins followed by an iterative process decreasing the number of bins until each bin had at least one data value. Variations in methods of estimating the pdf of daily streamflow lead to corresponding variations in resulting estimates of Q_e. We introduce a nonparametric kernel density method for estimating the pdf of daily streamflow that leads to a more consistent and reproducible determination of Q_e.

Given the wide variation associated with the definition and interpretation of Q_e as well as methods for its computation, one of our primary goals is to clarify its meaning and to introduce a consistent, reproducible, and objective method for its calculation. A secondary goal is to explore relationships among the sediment load carrying capacities of rivers across the United States and to introduce a generalized graphical approach for representing the frequency and magnitude of sediment loads and their associated streamflow discharges. Cross comparisons among rivers across the United States enable an improved understanding of the frequency and magnitude of both Q_e and $Q_{1/2}$.

Kernel Density Estimation of the Effective Discharge

We begin by introducing an empirical kernel density methodology for calculating effective discharge that eliminates existing inconsistencies in estimation of Q_e. These inconsistencies result from the numerous computational approaches presented in previous studies. All of the methods discussed in this article are tested and evaluated using suspended sediment data from the U.S. Geological Survey (USGS); thus, we begin by introducing the databases employed here.

Suspended Sediment and Discharge Data. Sediment and discharge data was provided by the U.S. Geological Survey (2007), which maintains a long-term continuous daily suspended sediment and discharge database across the United States. Daily suspended sediment loads L are computed from

$$L = QC, \tag{1}$$

where Q and C are daily discharge and suspended sediment concentration, respectively. For further information regarding suspended sediment sampling locations, sampling equipment, methodology, and lab analysis, see Guy (1969), Porterfield (1972), and Edwards and Glysson (1999).

For a data set to be representative of the behavior of sediment transport over a long period of time, it is important that it contain both frequent and less intense floods as well as the less frequent and more intense flood events. We considered all 62 USGS sampling locations with continuous consecutive daily suspended sediment records of 20 yr or longer as of 2007. These 62 sites are only a small fraction of the existing 1602 sites for which USGS provides suspended sediment and streamflow data (U.S. Geological Survey 2007).

From the available 62 sites with 20 or more years of record of suspended sediment and discharge data, a subset of 15 sites was selected to evaluate our proposed methodology for calculating Q_e. In addition, three of the 15 selected sites are highlighted to discuss our proposed empirical methodology in detail. The subset of 15 sites was chosen to be representative of all types of rivers throughout the United States on the basis of an analysis of the statistical characteristics of suspended sediment load data at all 62 sites described below.

Statistical Characteristics of Suspended Sediment Load across the United States. To improve our understanding of the behavior of suspended sediment loads, a simple theoretical model termed the "power law model" is useful. We emphasize that
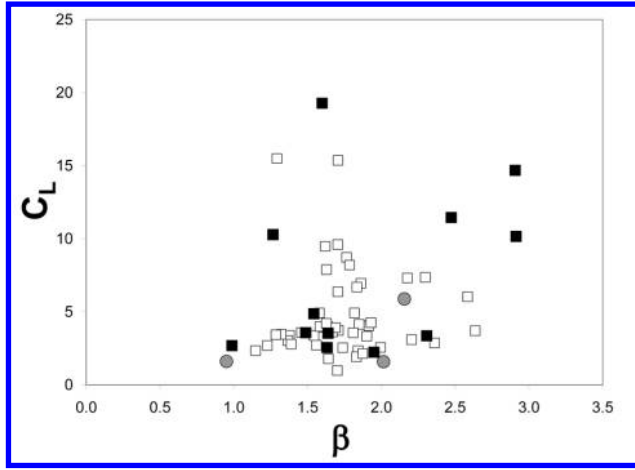
Figure 1. Coefficient of variation of load (C_L) versus power law exponent β for 62 USGS sites. Circles represent three sites used in detailed examples shown in figures 3–9, and circles and solid squares represent the subset of 15 sites described in tables 1 and 2.

the power law model is introduced here only to enable general comparisons among river sediment load behavior. We are not advocating the use of the simple power law model for any other purposes, such as for load estimation or estimation of discharge indices.

A power law is often a good first approximation of the relationship between the sediment load and discharge in a fluvial system (see, e.g., Nash 1994; Vogel et al. 2005):

$$L = e^{\alpha} Q^{\beta} e^{\varepsilon}, \tag{2}$$

where α and β are model parameters and ε is normally distributed model errors with zero mean and constant variance s_{ε}^2. Taking the natural logs in equation (2) yields

$$\ln(L) = \alpha + \beta \ln(Q) + \varepsilon. \tag{3}$$

The model parameters α and β are easily obtained from ordinary least squares regression between $\ln(L)$ and $\ln(Q)$. Since the power law model is fit in log space, to estimate L it is necessary to transform the model back into real space by exponentiation of equation (3), which is known to introduce transformation bias (Ferguson 1986). For this reason, a bias correction factor (BCF) is needed, as shown in equation (4), to ensure that the real space model does not generate biased loads:

$$L = e^{\alpha} Q^{\beta} \mathrm{BCF}. \tag{4}$$

We employ the BCF introduced by Ferguson (1986):

$$\mathrm{BCF} = \exp\!\left(\frac{s_{\varepsilon}^2}{2}\right), \tag{5}$$

where s_{ε}^2 is the variance of the residuals in equation (3). In general, the BCF is always greater than unity, and its value increases as the correlation between $\ln(L)$ and $\ln(Q)$ decreases and as β increases. See figure 3 of Vogel et al. (2005) for generalized relationships describing the behavior of the BCF for power law models, and see Cohn et al. (1989) for other methods for estimation of the BCF.

An important feature of the power law model for sediment loads is that it enables a generalized understanding of the approximate statistical behavior of L, C, and Q as a function of the model parameter β and other statistical summary statistics, such as the correlation between $\ln(L)$ and $\ln(Q)$, which we term ρ. We begin by exploring the variability of the loads, discharges, and the power law exponent β for the 62 rivers in figures 1 and 2. We summarize variability using the coefficient of variation of the discharges, C_Q, and the coefficient of variation of the loads, C_L. The coefficient of variation of a variable is simply its standard deviation divided by its mean. Figures 1 and 2 document that the variability of loads is often nearly an order of magnitude greater than the variability of the discharges. Acknowledging the extraordinary variability of loads evidenced by values of C_L often in excess of 5 is ex-
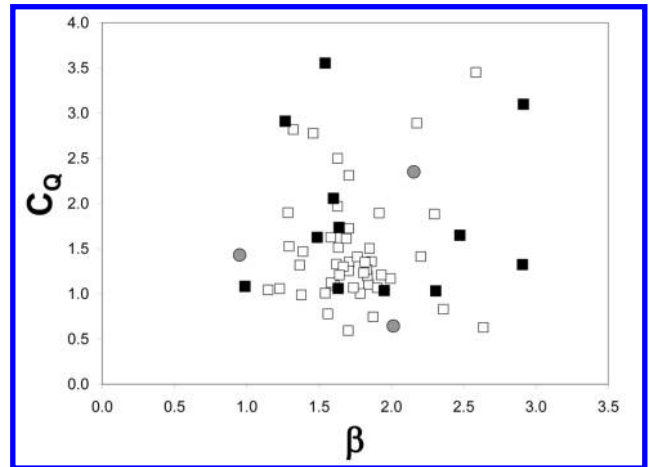

Figure 2. Coefficient of variation of discharge (C_Q) versus β for 62 USGS sites. Circles represent three sites used in detailed examples shown in figures 3–9, and circles and solid squares represent the subset of 15 sites described in tables 1 and 2.

tremely important. The enormous values of C_L documented in figure 1 emphasize the need for statistical models for representing sediment load behavior.

Using figures 1 and 2, a subset of 15 sites was selected to be representative of all U.S. rivers by capturing a broad range and combination of values of β, C_L, and C_Q. We also considered variations in the values of ρ and the length of record in selecting the 15 sites. Information about those 15 rivers is summarized in table 1, including their location, record length, drainage area, as well as values of the power law exponent β, the coefficient of variation of streamflow (C_Q) and of suspended sediment loads (C_L), and the correlation ρ between $\ln(Q)$ and $\ln(L)$. Though most of the rivers summarized in table 1 are large, we note that the characteristics of their sediment load behavior appear independent of the size of the rivers, so that, for example, rivers with extremely variable loads (large C_L) can exhibit both large and small drainage areas. Another interesting feature depicted in both table 1 and figures 1 and 2 is that the four statistical characteristics—β, C_Q, C_L, and ρ—behave independent of each other, so that increases (or decreases) in one of those characteristics do not generally imply increases (or decreases) in any of the others. This is true in spite of the fact that there exists an exact theoretical relationship between all four characteristics, as shown by Vogel et al. (2005, their eqq. [7], [14]).

Estimation of the Effective Discharge. Here we describe our proposed methodology for computing Q_e for a subset of three of the 15 sites for which the proposed methodology was used to compute Q_e. The three sites were the Mississippi, San Joaquin, and Eel rivers, which are marked by circles in fig-

ures 1 and 2. These three sites were selected because they encompass a broad range of values of β, C_Q, and C_L, summarized in table 1 and figures 1 and 2. The fitted power law model in equation (3) is shown in figure 3 for the three sites. The San Joaquin River produced an unusually low value of $\beta = 0.95$. Values of β are normally larger than unity and often much larger, as shown in table 1 and figures 1 and 2. The unusually low value of β for this river probably results from the relatively poor fit of the power law model for that site, as shown in figure 3.

Effective discharge, Q_e, has been loosely defined as the discharge that transports the most amount of sediment over time. Thus, Q_e is influenced by both discharge frequency and load carrying capacity. We use an empirical approach to calculate Q_e. Wolman and Miller (1960) introduced the idea of transport effectiveness $e(Q)$, defined as

$$e(Q) = L(Q)f_Q(Q), \qquad (6)$$

where $L(Q)$ represents the sediment load as a function of discharge Q and $f_Q(Q)$ represents the pdf of daily streamflow. The discharge that maximizes $e(Q)$ is termed the "effective discharge." A nonparametric empirical approach for computing and maximizing $e(Q)$ is described below. Nonparametric approaches are attractive because they do not depend on any model assumptions.

Maximizing transport effectiveness, $e(Q)$, to calculate Q_e requires an estimate of $f_Q(Q)$. Most previous studies have used histograms to approximate $f_Q(Q)$ (see, e.g., Hudson and Mossa 1997; Biedenharn et al. 1999; Sichingabula 1999; Crowder and Knapp 2005). Histograms are attractive for visualizing the frequency distribution of a data set; how-

Table 1. Background Information on 15 Rivers Considered

River name	Location	Record length (yr)	Drainage area (km²)	β	C_Q	C_L	ρ
Mississippi River	Missouri	46	251,229	2.01	.64	1.59	.865
San Joaquin River	California	31	35,058	.95	1.43	1.61	.893
Licking River	Kentucky	20	6024	1.49	1.62	3.57	.923
Eel River	California	21	8038	2.16	2.35	5.89	.975
Bad River	South Dakota	23	8047	1.54	3.55	4.87	.951
Rio Tanama	Puerto Rico	27	48	2.91	1.32	14.68	.836
Rio Grande floodway	New Mexico	36	71,743	.99	1.08	2.68	.734
Yadkin River	North Carolina	52	5905	2.31	1.03	3.36	.875
Green River	Utah	43	116,161	1.95	1.03	2.24	.814
Maumee River	Ohio	40	16,395	1.64	1.73	3.54	.959
Ralston Creek	Iowa	35	8	1.27	2.91	10.28	.860
Rio Grande Ottowa	New Mexico	37	37,037	1.63	1.06	2.55	.768
Trinity River	California	20	7389	2.47	1.64	11.45	.936
Feather River	California	23	9386	1.60	2.06	19.27	.940
Paria River	California	28	3652	2.91	3.10	10.16	.832

Note. Data include exponent β in equation (2), coefficient of variation of streamflow (C_Q) and load (C_L), and the correlation ρ between $\ln(Q)$ and $\ln(L)$.
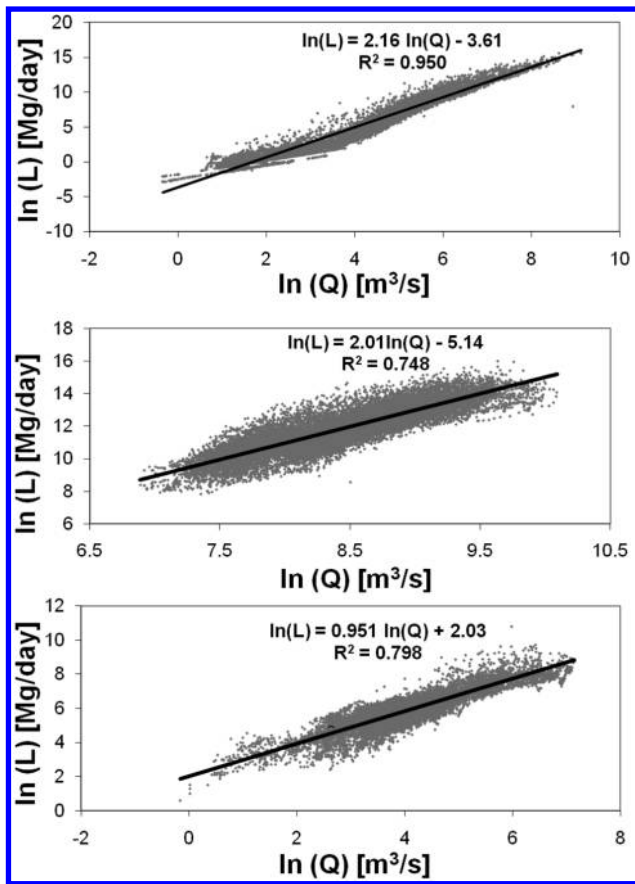
Figure 3. Sediment load rating curves for the Eel River (*top*), Mississippi River (*middle*), and San Joaquin River (*bottom*).

ever, their use for approximation of the pdf raises concerns generated by the need to define arbitrary bin sizes. With modern computational methods, the use of arbitrary bins is no longer necessary or attractive. Orndorff and Whiting (1999) raised similar concerns over inconsistencies in estimates of Q_e based on the use of histograms.

We recommend the use of a nonparametric kernel density approach to approximate the pdf of the discharges and loads. Lall (1995) reviews nonparametric function estimation methods, which are now in widespread use in the earth sciences. The kernel density approximation of loads and discharges was implemented with a Microsoft Excel add-in downloaded from the Analytical Methods Committee (AMC) website (Analytical Methods Committee 2007). This algorithm assumes a Gaussian kernel with a fixed-width smoothing parameter, h, around each data value used to generate the kernel density. Narrow windows created by small values of h produce jagged distributions.

Wide windows, or large values of the smoothing parameter h, produce smooth distributions (Silverman 1986). The Excel add-in optimizes for the smoothing parameter h on the basis of the mean integrated square error, with adjustments to consider bimodal distributions as well as heavily skewed data (Analytical Methods Committee 2007). The kernel density approximation of the pdf of daily streamflows mimics a histogram of the streamflows generated with a reasonable number of bins. By optimizing for the smoothing parameter h, inconsistencies that are caused by histogram binning are eliminated.

Estimates of Q_e vary when histograms are used, depending on the bin sizes selected. By utilizing the kernel density approximation of the pdf, Q_e will vary only with extreme deviations from the optimum smoothing parameter h. Figure 4 illustrates changes in Q_e with variations in the smoothing parameter h for the Eel River in Scotia, California. These changes are caused by variations in the smoothness of the transport effectiveness curve, as shown in figure 5 for the Eel River.

The kernel density approximation of the pdf depends on the choice of the smoothing parameter h. Changes in the kernel density approximation of the pdf caused by variations in the smoothing parameter h are shown in figure 6 and are compared with histograms with a consistent number of bins of the discharge data for the Eel River. In general, we recommend use of the optimal smoothing parameter to best represent the probability distribution of the data.

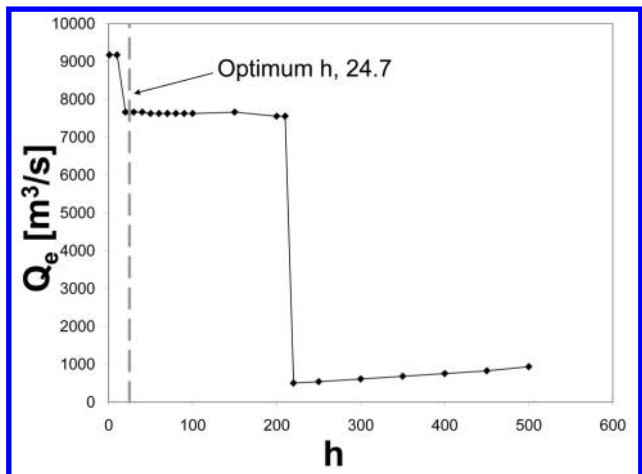Variability in estimates of the effective discharge

Figure 4. Changes in effective discharge Q_e with kernel density smoothing parameter h for the Eel River in Scotia, California.
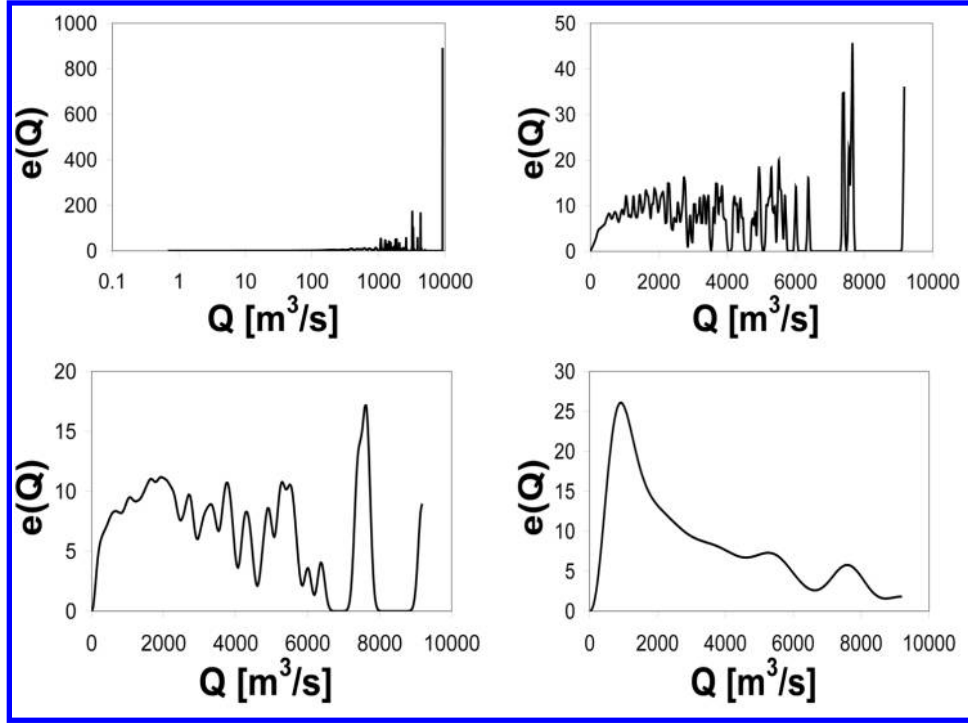
Figure 5. Transport effectiveness ($e(Q)$) curves with variations in the smoothing parameter h, with $h = 1$ (*top left*), $h_{optimal} = 24.7$ (*top right*), $h = 100$ (*bottom left*), and $h = 500$ (*bottom right*), for the Eel River in Scotia, California.

can also result from an inadequate number of discharge values selected to generate x, y pairs for plotting the pdf of discharge, as shown in figure 7 for the Eel River. Here we selected 256 equally spaced discharge values to develop each discharge pdf, which still results in a slight variability in estimates of Q_e; thus, we recommend selection of a larger number of discharge values in future studies.

Optimal kernel density approximations of the pdf's of daily streamflows are compared with histograms in figure 8 for the Mississippi, Eel, and San Joaquin rivers. Figure 8 demonstrates that the kernel density, when optimized for the smoothing parameter h, provides a nice approximation to the histogram of the discharge data for all three sites.

Figure 9 illustrates the transport effectiveness, $e(Q)$ given in equation (6) along with the effective discharge, Q_e, which is that discharge at which the $e(Q)$ is maximized for the Eel, Mississippi, and San Joaquin rivers. The transport effectiveness curves for the Mississippi and San Joaquin rivers shown in figure 9 are fairly smooth with obvious peaks, so in these cases there is a very natural effective discharge, Q_e. The Eel River, however, has multiple peaks, making the selection of a single maximum, Q_e, a subjective choice. Effective discharge, Q_e, is defined as that discharge that transports the most

sediment over time; however, as is shown in the case of the Eel River, there may be several discharges that transport the majority of sediment over time, making the selection of Q_e difficult and certainly not objective.

The multiple peaks associated with $e(Q)$ for the Eel River result from a few distinct properties of this river. The Eel River's relatively short record length combined with its high variability in both flow and load (i.e., high values of both C_Q and C_L) resulted in gaps in the $e(Q)$ relationship, because some discharge values were simply not experienced during the period of record for that river. This in turn creates a sharp drop in the pdf of streamflow (see fig. 8), which causes the jagged $e(Q)$ curve for the Eel River. In general, one expects other rivers with very high flow and load variability and short record lengths to produce similar $e(Q)$ curves, resulting in subjective and questionable estimates of Q_e.

The Half-Load Discharge Index

The half-load discharge, $Q_{1/2}$, was introduced by Vogel et al. (2003) as the discharge above and below which half of the total sediment load has been transported over time. Vogel et al. (2003) docu-
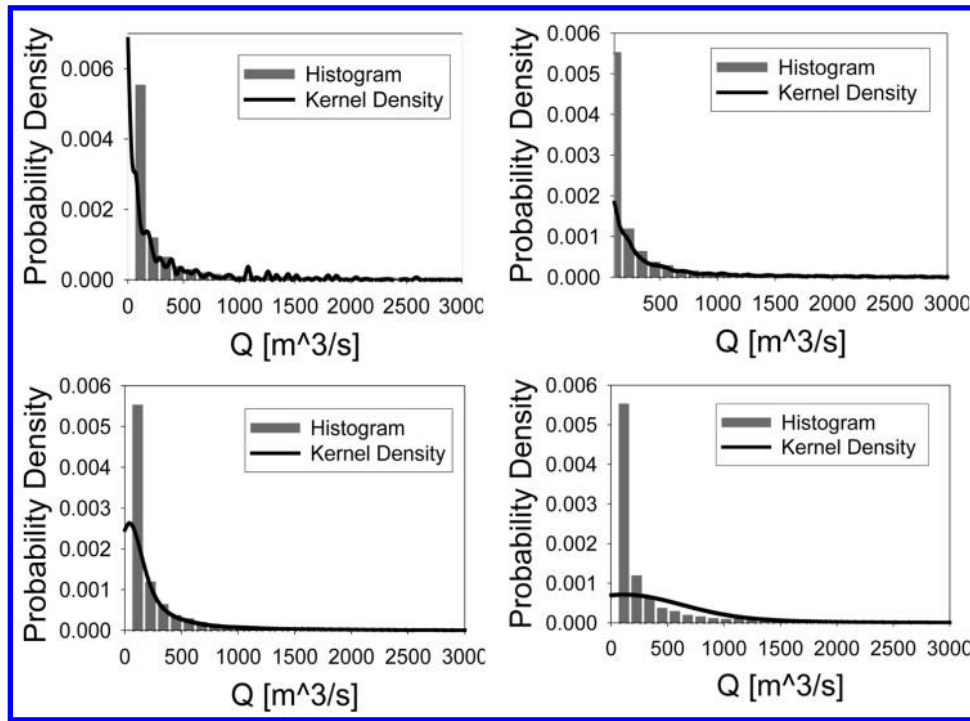
Figure 6. Kernel density approximations of probability distributions of daily streamflows compared with histograms with consistent bin sizes, with variations in the smoothing parameter h, with $h = 1$ (*top left*), $h_{optimal} = 24.7$ (*top right*), $h = 100$ (*bottom left*), and $h = 500$ (*bottom right*), for the Eel River in Scotia, California.

ments that $Q_{1/2}$ can be a very useful and easy to compute discharge index to augment our understanding of the amount of sediment transported by a particular river. We describe here how $Q_{1/2}$ can be used, along with Q_e, to better understand the behavior of sediment transport.

We recommend an empirical or nonparametric approach to estimation of $Q_{1/2}$ that does not depend on any model assumptions. First, the discharge data and their associated loads are sorted (by discharge in ascending order) for the entire period of record. The summation of the total load for the period of record is then used to generate the cumulative percent of suspended sediment load carried by each discharge in ascending order. The associated discharge at which 50% of the total cumulative sediment load had been transported is termed $Q_{1/2}$. Naturally, any fraction of total load, f, may be used other than the load fraction $f = 1/2$. Interestingly, the study by Vogel et al. (2003) was not the only study to introduce estimates of Q_f. For example, Hudson and Mossa (1997) and Sichingabula (1999) reported values of $Q_{1/2}$ or Q_f, although they did not advocate its use as an overall discharge index as did Vogel et al. (2003).

Graphical Summary of Frequency and Magnitude of Sediment and Discharge Behavior

Although the discharge indices Q_e and $Q_{1/2}$ are useful for describing sediment transport in a fluvial
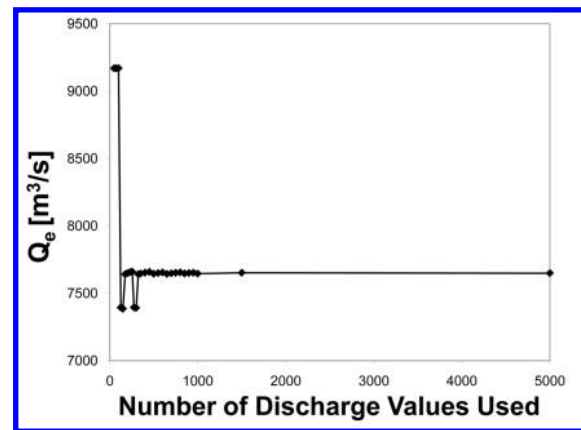

Figure 7. Example of variability in Q_e, with the number of discharge values used to generate a kernel density probability distribution function of the discharge data for the Eel River in Scotia, California.
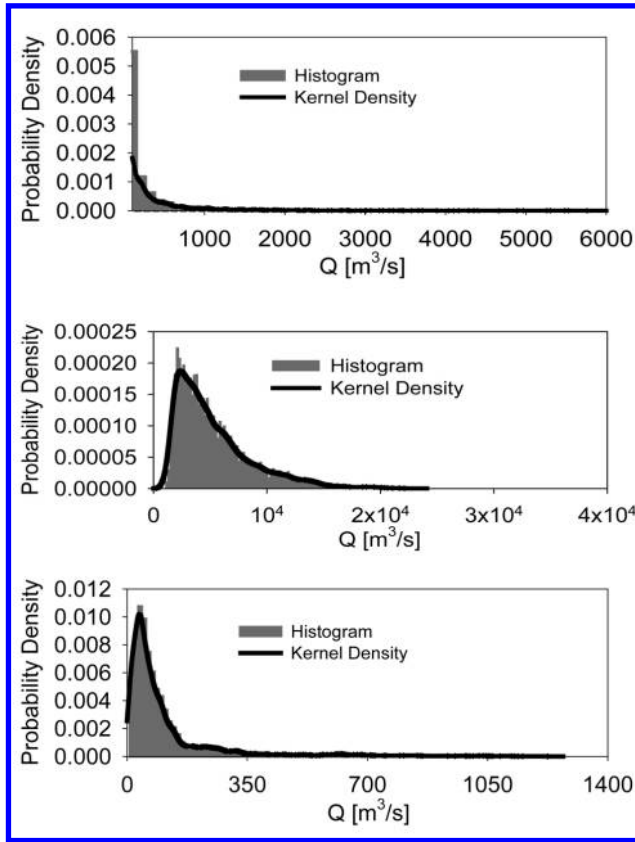
Figure 8. Comparisons between histograms and kernel density approximations of discharge data for the Eel River ($h = 24.7$; *top*), Mississippi River ($h = 395$; *middle*), and San Joaquin River ($h = 8.63$; bottom).

system, these indices do not fully describe the behavior of the magnitude and frequency of sediment and discharge data. Here we show how one can graphically display Q_e and $Q_{1/2}$ relative to other properties of a river's sediment-discharge relationship to enable a richer and more complete understanding of the behavior of sediment loads. To complement the discharge indices Q_e and $Q_{1/2}$, we recommend reporting summary plots that illustrate the cumulative distributions of the volume and time of occurrence associated with both sediment load and fluvial discharge. Such figures summarize the overall behavior of sediment and discharge using two separate plots: one for sediment loads and another for river discharges. These proposed plots also show the effective discharge Q_e and the half-load discharge $Q_{1/2}$, as well as additional sediment and discharge data.

Figures 10–12 show the summary plots of the San Joaquin, Eel, and Mississippi rivers, respectively. In each summary figure, the upper plot illustrates a

relative frequency curve of discharge data generated by the kernel density approximation, a curve indicating the cumulative fraction of nonexceedance time associated with each discharge, and a curve indicating the cumulative fraction of water (volume) carried by each daily discharge. Below each plot summarizing the river discharge data is a similar plot summarizing behavior of the sediment load data. These plots contain a relative frequency curve of the suspended sediment load, the cumulative fraction of sediment load carried by each discharge, and the cumulative fraction of nonexceedance time of the discharge associated with each sediment load. The discharge indices Q_e and $Q_{1/2}$ are also highlighted in the plots to enable evaluations of the relationship between these indices and the overall sediment transport for each fluvial system.

Figures 10–12 highlight differences in the behavior of sediment load and discharge data and, importantly, how these differences are not readily ap-
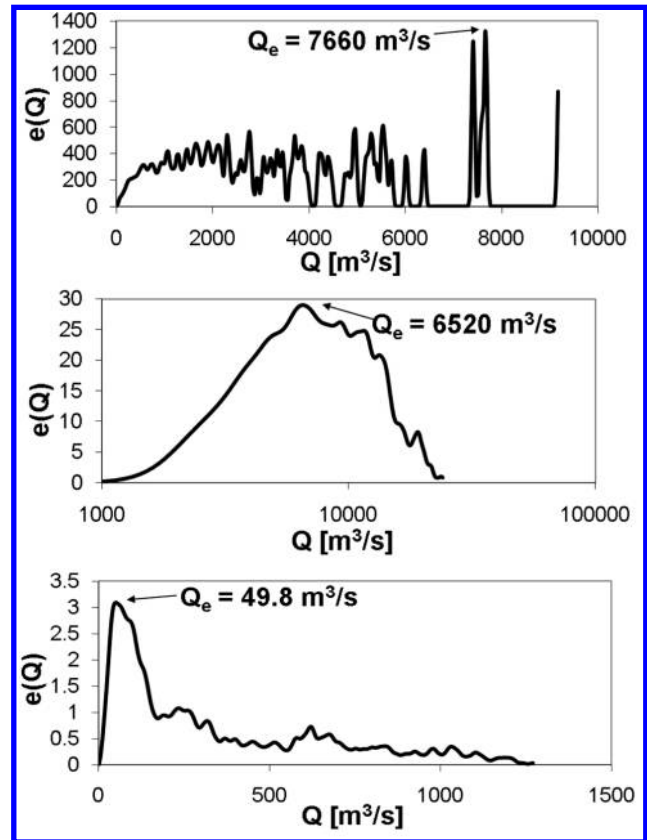

Figure 9. Transport effectiveness curves for the Eel River ($Q_e = 7660$ m³ s⁻¹; *top*), Mississippi River ($Q_e = 6520$ m³ s⁻¹; *middle*), and San Joaquin River ($Q_e = 49.8$ m³ s⁻¹; *bottom*).
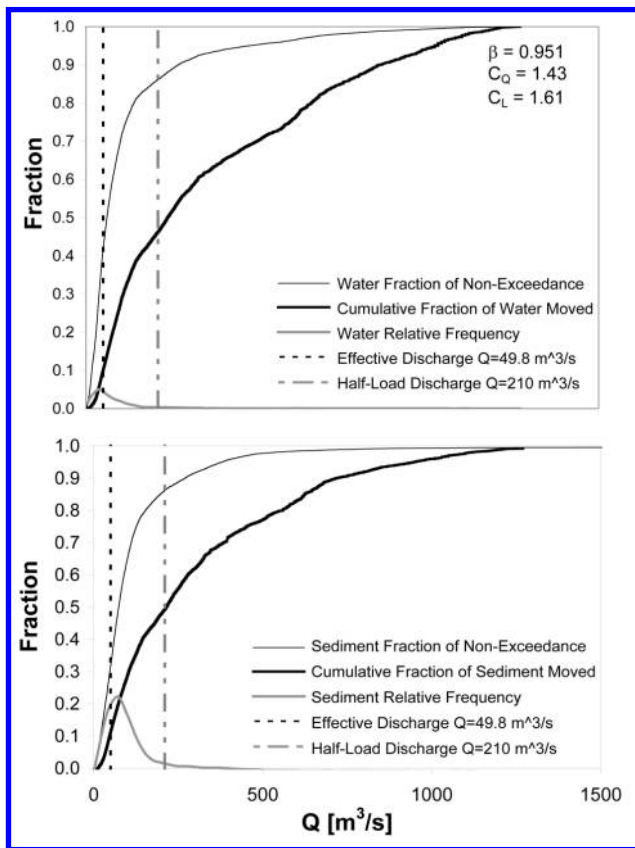
Figure 10. *Top*, water summary plot showing the cumulative fraction of flow nonexceedance, the cumulative fraction of total water volume per time moved, and the flow frequency distribution. *Bottom*, sediment summary plot showing the nonexceedance of flow associated with a given sediment transport volume based on the power law relationship, the cumulative fraction of total sediment moved relative to its associated flow based on the power law relationship, and the frequency distribution of the flow associated with sediment transport for the San Joaquin River.

parent from knowledge of the discharge indices Q_e or $Q_{1/2}$ (or both). These summary plots augment the information provided by both Q_e and $Q_{1/2}$ by showing their behavior relative to the distribution in volume and time of other discharges and loads.

Of particular interest in figures 10–12 is the wide variation in the fraction of the overall sediment load carried by discharges below Q_e. On the Eel River, discharges smaller than Q_e are responsible for carrying the majority of the total sediment load (97.8%), whereas on the Mississippi and San Joaquin rivers, discharges smaller than Q_e are responsible for carrying less than one-third of the total sediment load. Estimates of the two discharge indices Q_e and $Q_{1/2}$ for the 15 sites listed in table 1

are summarized in table 2. Also shown in table 2 are the mean daily streamflow, μ_Q, as well as the percentage of time and volume of sediment carried by flows in excess of Q_e. Table 2 documents that both the fraction of sediment load carried by discharges less than Q_e as well as their exceedance probabilities can vary dramatically across rivers. Even though Q_e is widely considered to be the discharge value that carries the most sediment over time (and flows in its neighborhood), it is possible that all river discharges less than Q_e may carry only a very small volume of sediment relative to the total sediment load. Furthermore, flows less than Q_e carry widely varying amounts of sediment from one river to another. For these reasons, we question

Figure 11. *Top*, water summary plot showing the cumulative fraction of flow nonexceedance, the cumulative fraction of total water volume per time moved, and the flow frequency distribution. *Bottom*, sediment summary plot showing the nonexceedance of flow associated with a given sediment transport volume based on the power law relationship, the cumulative fraction of total sediment moved relative to its associated flow based on the power law relationship, and the frequency distribution of the flow associated with sediment transport for the Eel River.
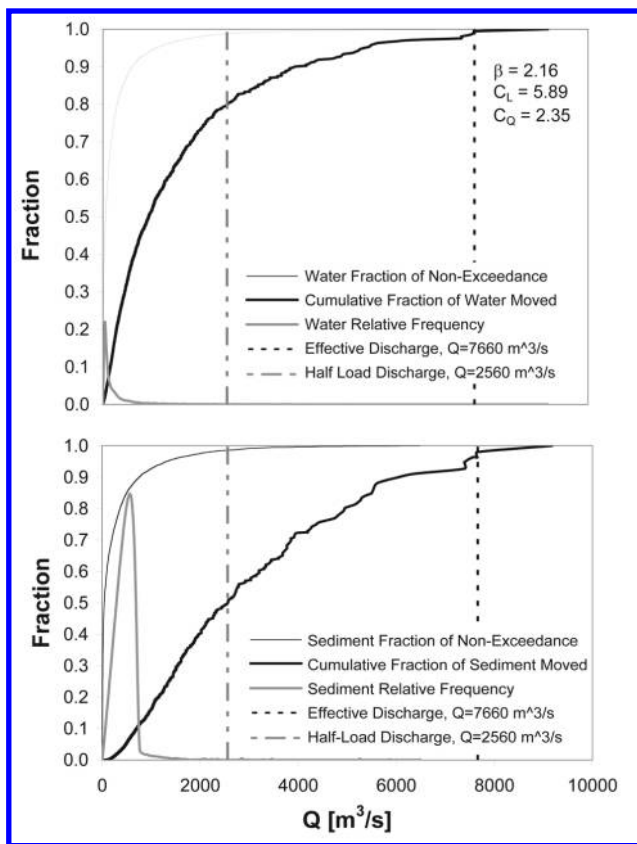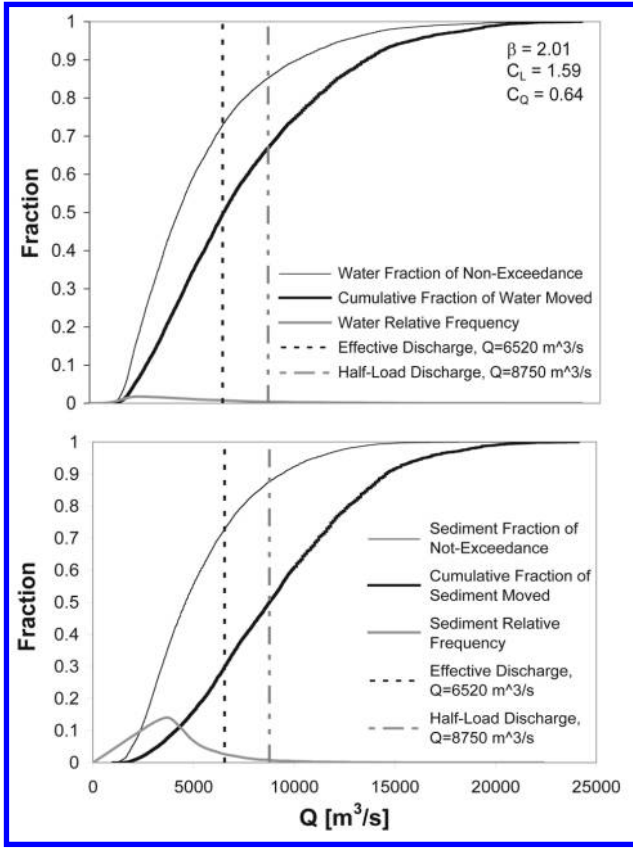
Figure 12. *Top*, water summary plot showing the cumulative fraction of flow nonexceedance, the cumulative fraction of total water volume per time moved, and the flow frequency distribution. *Bottom*, sediment summary plot showing the nonexceedance of flow associated with a given sediment transport volume based on the power law relationship, the cumulative fraction of total sediment moved relative to its associated flow based on the power law relationship, and the frequency distribution of the flow associated with sediment transport for the Mississippi River.

the use of Q_e as the singular measure of a river's ability to transport sediment over the long term.

Figures 10–12 provide a wealth of information concerning the frequency and magnitude of both river discharges and sediment loads. Of particular interest to this study is the location of Q_e and $Q_{1/2}$ relative to each other and relative to the overall distributions of the volume and time of occurrence for the sediment and water. For both the Mississippi and the San Joaquin rivers, Q_e is a relatively small flow with exceedance probabilities of 27% and 59%, respectively, as predicted by Wolman and Miller (1960) and others. However, Q_e for the Eel River is a large flood event that was exceeded only

0.1% of the time, reinforcing the concept of the Eel River being dominated by infrequent and large flood events. Furthermore, Q_e is larger than $Q_{1/2}$ for the Eel River, whereas the reverse is true for both the Mississippi and the San Joaquin rivers. This result reinforces the need to view both Q_e and $Q_{1/2}$ within the context of the entire distributions of sediment and discharges, as shown in the summary plots in figures 10–12.

Theoretical Relations among Discharge Indices

Here we discuss theoretical relationships among Q_e and $Q_{1/2}$; however, we stress that we do not recommend such approaches for estimation of such discharge indices, only for improving our understanding of their behavior and to enable cross river comparisons. Goodwin (2004) derived theoretical relations for Q_e corresponding to the normal, gamma, two- and three-parameter lognormal, Pearson Type III, and log Pearson Type III distributions of daily streamflow. Quader et al. (2008) provide similar results for a mixed exponential distribution for use in small intermittent streams in Ontario, Canada. Vogel et al. (2003) focus on the lognormal distribution and point out that the expressions derived by Nash (1994) for Q_e corresponding to the lognormal distribution used a different definition of Q_e than that introduced originally by Wolman and Miller (1960). Vogel et al. (2003) also show that the equation derived by an analysis of Q_e by Nash (1994) actually calculates $Q_{1/2}$ rather than Q_e. Goodwin (2004, 2006) and Quader et al. (2006) provide further discussions and corrections for the lognormal case. Similarly, Vogel et al. (2003) derived the following expressions for both Q_e and $Q_{1/2}$ when discharge, sediment concentrations, and sediment loads follow a two-parameter lognormal distribution and when the sediment loads follow the power law model in equation (2):

$$Q_{1/2} = \mu_Q(1 + C_Q^2)^{\beta - 0.5}, \tag{7a}$$

$$Q_e = \mu_Q(1 + C_Q^2)^{\beta - 1.5}, \tag{7b}$$

where μ_Q is the average daily discharge, C_Q is the coefficient of variation of the daily discharges, and β is the exponent in the power law model in equation (2).

Equations (7) imply that for plausible values of β ($\beta > 0.5$), one expects $Q_{1/2}$ to always exceed μ_Q, which is always consistent with our empirical results reported in table 2. Equations (7) also imply that Q_e will exceed μ_Q when $\beta > 1.5$ and that Q_e will be less than μ_Q when $\beta < 1.5$. Interestingly,

Table 2. Properties of Q_e and $Q_{1/2}$ for 15 Selected Rivers along with the Mean Daily Streamflow μ_Q

River name	μ_Q (m³ s⁻¹)	Q_e (m³ s⁻¹)	$Q_{1/2}$ (m³ s⁻¹)	Time Q_e was exceeded (%)	Sediment volume carried by flows ≤Q_e (%)
Mississippi River	5316	6520	8750	27.0	29.8
San Joaquin River	117.3	49.8	210	58.4	11.6
Licking River	84.3	251	396	9.46	28.8
Eel River	244.3	7660	2560	.03	97.9
Bad River	8.2	328	78.4	.17	92.6
Rio Tanama	1.3	56.6	9.03	.01	100
Rio Grande floodway	36.8	24.9	67.7	47.2	17.1
Yadkin River	85.0	89.6	239	26.8	13.3
Green River	171.4	491	425	7.07	59.1
Maumee River	146.4	377	784	11.5	16.7
Ralston Creek	.08	.0415	1.10	35.9	.96
Rio Grande Ottowa	40.9	25.5	80.1	21.1	34.5
Trinity River	142.4	4760	1170	.02	100
Feather River	87.7	92.8	1750	25.2	1.05
Paria River	.76	69.7	14.2	.01	100

both of these conditions on Q_e hold for all 15 rivers except for the Rio Grande in Ottawa, where $Q_e < \mu_Q$ yet $\beta = 1.65$. Equations (7) imply that the ratio of $Q_{1/2}/Q_e$ will always equal $1 + C_Q^2$; thus, $Q_{1/2}$ should always exceed Q_e. However, table 2 indicates that $Q_e > Q_{1/2}$ for only nine of the 15 rivers considered. Clearly the theoretical model is useful for helping us to understand the factors that influence the behavior of these two discharge indices. However, the theoretical model is based on a lognormal model of flows and a power law model relating flows and loads. Both of these models are only crude approximations to reality; hence, empirical findings are preferred over the theoretical model.
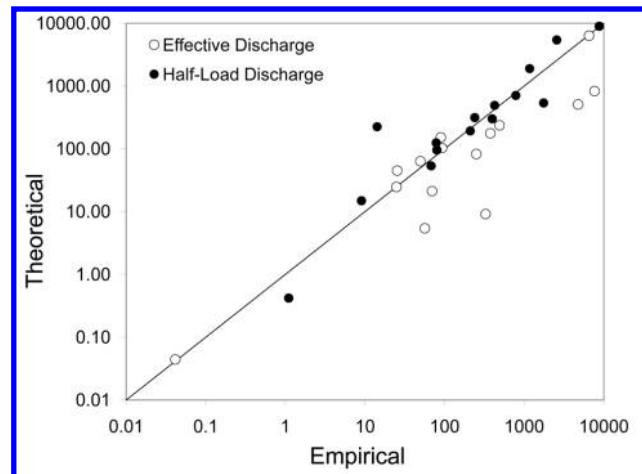
Figure 13 compares the theoretical values for Q_e and $Q_{1/2}$ obtained from equations (7) with the empirical estimates of those same statistics for 15 rivers chosen to be representative of rivers across the United States. We conclude from figure 13 that for these selected rivers, the lognormal pdf of flow combined with the power law model of loads can provide only a very crude approximation to either Q_e and/or $Q_{1/2}$.

We have found, as did Archfield (2009), that a lognormal pdf can provide only a very rough approximation to the distribution of daily streamflow, with large deviations often occurring at both high and low discharges. More complex models are needed to approximate the daily discharge distribution. Even the three-parameter distributions considered by Goodwin (2004) are unlikely to fit very well on the basis of the findings of Archfield (2009). Still, we have shown that the theoretical lognormal model of discharge combined with the power law

model of sediment loads can provide important insights into the sediment load transport problem.

Regional Relations among Discharge Indices

Many previous studies have sought to improve our understanding of how the frequency and magnitude of effective discharge varies from one river to another. Here we explore the ability of the theoretical relationships for Q_e and $Q_{1/2}$ to improve our understanding of variations in those statistics across sites. Consider the normalized versions of equations (7):

Figure 13. Comparison of empirical and theoretical values of effective and half-load discharges.
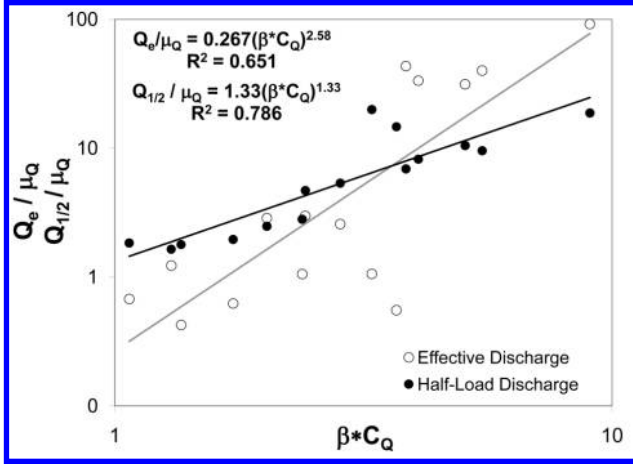
Figure 14. Relationships between empirical values of normalized effective discharge (Q_e/μ_Q), normalized half-load discharge $(Q_{1/2}/\mu_Q)$, and the coefficient of variation of discharge (C_Q) and the power law exponent (β).

$$\ln\left(\frac{Q_{1/2}}{\mu_Q}\right) = (\beta - 0.5)\ln(1 + C_Q^2), \qquad (8a)$$

$$\ln\left(\frac{Q_e}{\mu_Q}\right) = (\beta - 1.5)\ln(1 + C_Q^2). \qquad (8b)$$

We hypothesize that even though the lognormal and power law models can provide only a rough approximation to the behavior of sediment loads, equations (8) document that variations in both Q_e and $Q_{1/2}$ depend largely on variations in both β and C_Q. To test this hypothesis, figure 14 compares empirical values of Q_e/μ_Q and $Q_{1/2}/\mu_Q$ with values of the product of β and C_Q for each of the 15 rivers.

Figure 14 documents that both C_Q and β appear to explain a good deal of the variability in the normalized values of Q_e and $Q_{1/2}$. The resulting regressions shown in figure 14 could be used to approximate both Q_e and $Q_{1/2}$ for any river, given estimates of μ_Q, C_Q, and β. Reliable estimates of μ_Q are available for any river in the United States from the multivariate relationships developed by Vogel et al. (1999). The regressions in figure 14 are based on data from only 15 sites. It is expected that an expansion of these relationships with data from more sites would provide a more accurate explanation of the variability in normalized values of Q_e and $Q_{1/2}$.

Similar relationships were developed using theoretical values of Q_e and $Q_{1/2}$ based on equations (7) that are not presented in this article. Klonsky (2008) showed that in many instances the two-parameter log normal distribution was a poor approximation to the pdf of daily streamflow, and this in part caused the theoretical model to perform poorly in some cases.

Quader and Guo (2009) performed a sensitivity analysis of Q_e for small urban streams in southern Ontario and found that Q_e was largely influenced by the value of β and the coefficient of variation of the streamflow, similar to the findings reported in figure 14. Additionally, Quader and Guo (2009) found the skewness coefficient of streamflow and a flashiness index of the streamflow to influence the value of Q_e.

Sichingabula (1999) developed expressions that related values of Q_e to basin drainage basin area. For the 15 basins considered here, the correlation between Q_e and drainage basin area was only 0.170. We do not expect values of Q_e to depend on drainage area alone. Instead, equations (7b) and (8b) suggest that in addition to the mean streamflow, Q_e will depend on characteristics that govern the behavior of the pdf of streamflow C_Q and the power law model β, which are not generally related to basin scale.

Of equal interest is our ability to predict the frequency of the various discharge indices. Figure 15 documents good relationships between the normalized values of Q_e and $Q_{1/2}$ and their corresponding exceedance probabilities. As the normalized Q_e and $Q_{1/2}$ increase, their exceedance probability decreases, and approximate relationships are given in figure 15.
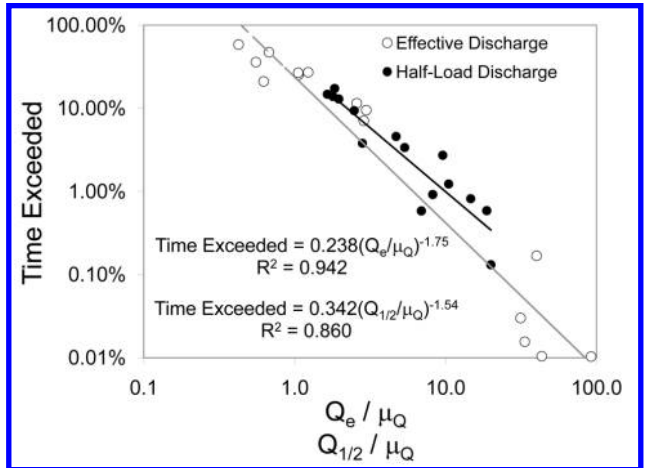

Figure 15. Normalized Q_e and $Q_{1/2}$ versus frequency of exceedance.

Conclusions

The concept of effective discharge, Q_e, was introduced by Wolman and Miller (1960) as that stream discharge that transports the most sediment over time. Recently, the validity of Q_e as an overall descriptor of sediment transport has been questioned, and new discharge indices—such as the half-load discharge, $Q_{1/2}$—have been introduced. We used long-term continuous daily suspended sediment and discharge data collected throughout the United States to explore the empirical behavior of Q_e and $Q_{1/2}$. We selected 15 rivers expected to be representative of the complete range of behavior of suspended sediment loads across the United States. The following conclusions were reached.

1. A more consistent method of estimating the effective discharge Q_e is introduced that is based on a kernel density approximation of the probability density of daily discharges and loads. This approach is more objective and reproducible than previous approaches that employ bins of arbitrary width to construct histograms.

2. Figures 10–12 are a key contribution and recommendation of this study because they provide a graphical approach for representing and understanding relationships between the magnitude and frequency of both streamflow and suspended sediment loads. These summary plots enable a comprehensive evaluation of the frequency and magnitude of the discharge indices Q_e and $Q_{1/2}$ in terms of both their frequency of occurrence and the fraction of loads that they carry. These figures show clearly that the fraction of sediment carried by discharges smaller than Q_e can vary dramatically from one river to another, raising questions regarding the overall meaning and value of Q_e as a discharge index.

3. Similar to Vogel et al. (2005) and many other studies, we have found that a power law regression model provides a rough approximation to the relationship between sediment loads and river discharge. Similar to Archfield (2009) and others, we

have also found that the distribution of daily discharges are more complex than any two- or three-parameter pdf, yet still the lognormal model of streamflow combined with a power law model of the load-flow relationship was shown to be useful for developing cross comparisons of the behavior of Q_e and $Q_{1/2}$. Across a wide spectrum of U.S. rivers, both Q_e and $Q_{1/2}$ are approximately related to the first two moments of daily river discharge as well as the power law exponent β in the sediment load-discharge relationship. We noted systematic variations in Q_e and $Q_{1/2}$ as a function of μ_Q, C_Q, and β, and empirical relationships were developed that enable estimation of these discharge indices as a function of μ_Q, C_Q, and β.

4. The theoretical model predicted that the $Q_{1/2}$ will always exceed μ_Q, and this result was consistent with our empirical findings at all 15 sites considered. The theoretical model predicted that Q_e will exceed μ_Q only when $\beta > 1.5$, and this result was also consistent with all of our empirical findings, with the exception of one of the 15 sites considered.

5. Empirical equations were developed that describe the relationship between normalized values of both Q_e and $Q_{1/2}$ and their exceedance probability. As the ratio of the normalized Q_e and $Q_{1/2}$ increased, the percent of time exceeded was shown to decrease systematically.

Overall, this study has sought to improve our understanding of the behavior of discharge indices and sediment load data for rivers across the United States. The study has led to improvements in our ability to estimate Q_e and, importantly, has shown that both discharge indices Q_e and $Q_{1/2}$ provide only a partial understanding of the behavior of sediment and discharge data for a particular river. The generalized summary plots shown in figures 10–12 are recommended in addition to the use of the discharge indices Q_e and $Q_{1/2}$ for explaining the overall behavior of sediment transport for a particular river.

REFERENCES CITED

Analytical Methods Committee. 2007. Analytical Methods Committee software. http://www.rsc.org/Membership/Networking/InterestGroups/Analytical/AMC/Software/kerneldensities.asp.

Archfield, S. A. 2009. Estimation of continuous daily streamflow at ungaged locations in southern New England. PhD dissertation, Tufts University, Medford, MA.

Biedenharn, D. S.; Thorne, C. R.; Soar, P. J.; Hey, R. D.;

and Watson, C. C. 1999. A practical guide to effective discharge calculation. *In* Watson, C. C.; Biedenharn, D. S.; and Thorne, C. R., eds. Demonstration erosion control: design manual. Vicksburg, MS, Engineer Research and Development Center, U.S. Army Corps of Engineers, p. 239–274.

Bledsoe, B. P.; Brown, M. C.; and Raff, D. A. 2007. Geotools: a toolkit for fluvial system analysis. J. Am. Water Res. Assoc. 43:757–772.

Cohn, T. A.; DeLong, L. L.; Gilroy, E. J.; Hirsch, R. M.; and Wells, D. K. 1989. Estimating constituent loads. Water Resour. Res. 25:937–942.

Crowder, D. W., and Knapp, H. V. 2005. Effective discharge recurrence intervals of Illinois streams. Geomorphology 64:167–184.

Doyle, M. W., and Shields, C. A. 2008. An alternative measure of discharge effectiveness. Earth Surface Process. Landforms 33:308–316.

Doyle, M. W.; Stanley, E. H.; Strayer, D. L.; Jacobson, R. B.; and Schmidt, J. C. 2005. Effective discharge analysis of ecological processes in streams. Water Resour. Res. 41:1–16.

Edwards, T. K., and Glysson, G. D. 1999. Field methods for measurement of fluvial sediment. U.S. Geol. Surv. Techniques of Water-Resources Investigations Rep. Washington, DC, Government Printing Office, 89 p.

Ferguson, R. I. 1986. River loads underestimated by rating curves. Water Resour. Res. 22:74–76.

Goodwin, P. 2004. Analytical solutions for estimating effective discharge. J. Hydraulic Eng. 130:729–738.

———. 2006. Discussion of "Analytical solutions for estimating effective discharge." J. Hydraulic Eng. 132:114–115.

Guy, H. P. 1969. Laboratory theory and methods for sediment analysis. U.S. Geol. Surv. Techniques of Water-Resources Investigations Rep. Washington, DC, Government Printing Office, 59 p.

Hudson, P. F., and Mossa, J. 1997. Suspended sediment transport effectiveness of three large impounded rivers, U.S. Gulf Coast Plain. Environ. Geol. 32:263–273.

Klonsky, L. S. 2008. Effective measures of effective discharge. MS thesis, Tufts University, Medford, MA.

Lall, U. 1995. Recent advances in nonparametric function estimation: hydrologic applications. Rev. Geophys. 33:1093–1102.

Nash, D. B. 1994. Effective sediment-transporting discharge from magnitude-frequency analysis. J. Geol. 102:79–95.

Orndorff, R. L., and Whiting, P. J. 1999. Computing effective discharge with S-PLUS. Comput. Geosci. 25:559–565.

Porterfield, G. 1972. Computation of fluvial-sediment discharge. U.S. Geol. Surv. Techniques of Water-Resources Investigations Rep. Washington, DC, Government Printing Office, 66 p.

Quader, A., and Guo, Y. P. 2009. Relative importance of hydrological and sediment-transport characteristics affecting effective discharge of small urban streams in southern Ontario. J. Hydrol. Eng. 14:698–710.

Quader, A.; Guo, Y. P.; and Bui, T. 2006. Discussion of "Analytical solutions for estimating effective discharge." J. Hydraulic Eng. 132:112–114.

Quader, A.; Guo, Y. P.; and Stedinger, J. R. 2008. Analytical estimation of effective discharge for small southern Ontario streams. Can. J. Civil Eng. 35:1414–1426.

Sichingabula, H. M. 1999. Magnitude-frequency characteristics of effective discharge for suspended sediment transport, Fraser River, British Columbia, Canada. Hydrol. Process. 13:1361–1380.

Silverman, B. W. 1986. Density estimation for statistics and data analysis. London, Chapman & Hall, 175 p.

U.S. Geological Survey. 2007. USGS suspended-sediment database. http://co.water.usgs.gov/sediment.

Vogel, R. M.; Rudolph, B.; and Hooper, R. P. 2005. The probabilistic behavior of water quality loads. J. Environ. Eng. 131:1081–1089.

Vogel, R. M.; Stedinger, J. R.; and Hooper, R. P. 2003. Discharge indices for water quality loads. Water Resour. Res. 39:1273.

Vogel, R. M.; Wilson, I.; and Daly, C. 1999. Regional regression models of annual streamflow for the United States. J. Irrig. Drainage Eng. 125:148–157.

Wolman, M. G., and Miller, J. P. 1960. Magnitude and frequency of forces in geomorphic processes. J. Geol. 68:54–74.